

Polarization basis tracking scheme for quantum key distribution with revealed sifted key bits

Yu-Yang Ding^{1,2}, Wei Chen^{1,2,*}, Hua Chen³, Chao Wang^{1,2}, Ya-Ping li^{1,2},
Zhen-Qiang Yin^{1,2}, Shuang Wang^{1,2}, Guang-Can Guo^{1,2}, Zheng-Fu Han^{1,2}

¹ *Key Laboratory of Quantum Information, CAS,*

University of Science and Technology of China, Hefei 230026, China

² *Synergetic Innovation Center of Quantum Information and Quantum Physics,*

University of Science and Technology of China, Hefei, Anhui 230026, China

³ *China Aerospace Science and Technology Corporation*

**:Corresponding author: kooky@mail.usc.edu.cn*

(Dated: March 1, 2022)

Calibration of the polarization basis between the transmitter and receiver is an important task in quantum key distribution (QKD). An effective polarization-basis tracking scheme will decrease the quantum bit error rate (QBER) and improve the efficiency of a polarization encoding QKD system. In this paper, we proposed a polarization-basis tracking scheme using only unveiled sifted key bits while performing error correction by legitimate users, rather than introducing additional reference light or interrupting the transmission of quantum signals. A polarization-encoding fiber BB84 QKD prototype was developed to examine the validity of this scheme. An average QBER of 2.32% and a standard deviation of 0.87% have been obtained during 24 hours of continuous operation.

PACS numbers: 03.67.Dd, 03.67.Hk, 42.50.Ex

Quantum key distribution (QKD) could in principle implement information-theoretic security (ITS) key reconciliation using quantum mechanics. Since Bennett and Brassard proposed the most famous QKD protocol (BB84) in 1984[1], further advances have been made both in theory and experiment [2–4]. In most QKD experiments, photons are natural resources to carry quantum information, which can be transferred through fiber or free space channels. Fiber is the most widely used quantum channel profiting from its extensibility, while its birefringence has disturbed experimental researchers for many years. The birefringence of the fiber makes QKD systems vulnerable to environmental disturbance and significantly affects the performance of QKD systems. For example, the polarization reference frames of a transmitter Alice and a receiver Bob will be misaligned in polarization encoding QKD systems, which will directly increase the quantum bit error rate (QBER) of the system[5]. In phase encoding QKD systems, polarization fluctuation will reduce the fringe visibility and consequentially increase the QBER of the systems.[6, 7]. Due to its adverse effects, effective polarization compensation schemes should be performed in QKD systems.

Some passive self-compensation methods have been developed for phase encoding QKD systems, such as the "Plug-and-play" [8] and "Faraday-Michelson" [9] structures, while active feedback tracking is still a major methods used in polarization encoding QKD systems [5, 10–16]. Depending on whether it halts the quantum photon transmitting procedure, most of these strategies can be divided into two types, the interrupting scheme [5, 10–12] and the real-time scheme [13–15]. The former will apparently sacrifice the efficiency of the system. The latter is primarily based on the time-division multiplexing (TDM) and the wavelength-division multiplexing (WDM) methods. The TDM methods send the reference signals in the time intervals between quantum photons, which may not be compatible with up-to-date high-speed QKD systems. The WDM methods send reference signals with the wavelength distinct from the quantum signals, thus may limit the security transmission distance of QKD due to the polarization decorrelation between the two signals [11, 17]. Because most of these schemes need extra components such as photodetectors or laserdiodes, the QKD system will be more complicated and will need to be carefully designed to protect the quantum photons from the "pollution" of the relatively strong reference light.

In this paper, we propose a real-time continuous polarization-basis tracking scheme for QKD based on single photon detection signals. We use the sifted key bits unveiled and discarded during the post processing procedure of QKD, which are usually 10% to 20% of the total sifted key bits [2, 3, 18], to calculate the feedback control signals of a gradient algorithm that are applied to the polarization control (PC) components accordingly. Because the scheme can be implemented without extra photon sources, detectors and time expenditures, the method can be used in some single photon level quantum optical experiments[19, 20]. We applied the scheme to the off-the-shelf electronic polarization controllers (EPCs) in a typical polarization encoding QKD system to compensate for the polarization disturbance of a 50 km fiber channel. The polarization-basis tracking can be performed during the post-processing of QKD without interrupting the transmission of quantum signals. The average QBER of the QKD system is 2.32% and the standard derivation is 0.87% during 24 hours of continuous operation, which effectively verified the validity of using this method in QKD.

The polarization-basis tracking method should be used in conjunction with specific polarization control components in QKD systems. The EPCs based on fiber-squeezers [22] are fundamental devices used in QKD system profiting from their low insertion loss. Major drawbacks of this type of EPCs are low modulating rates and inconsistency even when the same driving voltages are applied. Thus, an optimizing algorithm should be developed to make them work efficiently. We selected the four-stage EPCs (PolaRITE III, General Photonics, 5228 Edison Avenue Chino, CA 91710) as the polarization control unit, which has an insertion loss as low as 0.05 dB. The EPC consists of four electronic fiber squeezers (FSs) X_1, X_2, X_3 and X_4 . The functions of X_3 and X_4 are the same as X_1 and X_2 , respectively. The voltage applied on one FS will rotate the state of polarization (SOP) with an angle of φ_i around the axis Ω_i ($i = 1, 2, 3, 4$) on the *Poincaré* sphere. The rotation \mathfrak{R}_i can be described by the Hamilton's *quaternion*[24]:

$$\mathfrak{R}_i = \cos \frac{\varphi_i}{2} + \sin \frac{\varphi_i}{2} \Omega_i \quad (1)$$

where φ_i is determined by the voltage v_i on the FS $_i$, and Ω_i represents the rotation axis on the *Poincaré* sphere. The SOP $|S_1\rangle$ after rotating an input state $|S_0\rangle$ with one squeezer can be represented by their normalized Stokes vectors S_0 and S_1 :

$$S_1 = \mathfrak{R}_i S_0 \mathfrak{R}_i^* \quad (2)$$

In principle, any SOP changing in the fiber channels can be compensated by driving the EPC with proper voltages. Three FSs are sufficient to track all polarization states and the algorithm can be made more flexible with extra FSs [23]. The driving voltages are adjusted according to the feedback signal E , which is a function of the current values of the driving voltages v_i and Ω_i ($i=1, 2, 3$, and 4). Unfortunately, the directions of the FS's rotation axes change over time due to their mechanical structures and environmental disturbances. As a result, there are two challenges to implementing a real-time polarization tracking algorithm with this type of EPCs: *a*) it is difficult to build a look-up

table for each squeezer and Ω_i must be measured each time before adjustment and, b) the algorithm works during quantum key transmission, which means it is unavailable to traverse all combinations of EPC driving voltages. To overcome these disadvantages, we modified the widely used Gradient algorithm according to the traits of EPC and QKD systems. The flow chart of the algorithm can be described as in algorithm 1.

Algorithm 1. The Gradient algorithm

```

1: procedure GRADIENT( $v_i, E$ )
2:    $v_i \leftarrow C_i$ 
3:    $i \leftarrow 1$ 
4:   calculate  $E$ 
5:   while  $E > E_{thr}$  do
6:      $E_1 \leftarrow E$ 
7:      $v_i \leftarrow v_i + D$ 
8:     calculate  $E$ , then  $E_2 \leftarrow E$ 
9:      $v_i \leftarrow v_i - D + \tau \times (E_2 - E_1) / D$ 
10:     $i \leftarrow i \bmod 4 + 1$ 
11:    calculate  $E$ 
12:  end
13:  back to step 3

```

In algorithm 1, $i=1,2,3$ and 4; C_i is the center of the normal range of v_i . The arrows \leftarrow represents the assignment operation, v_i is the immediate driving voltage on the EPC squeezer's axis Ω_i ($i=1,2,3$ and 4), E is the feedback value and E_{thr} is the threshold value of the deviation from the ideal situation in the QKD system. The parameter D is a small dither value and τ is an amplification factor of the voltage adjustment. At the beginning of the algorithm, the four v_i ($i = 1, 2, 3, 4$) were initialized as the center value of the dynamic range of the driving voltage. Because the rotation of Ω_i is slowly varying, it can be regarded as a constant from step 6 to step 11 within a cycle of the algorithm. To estimate the reference value of Ω_i , a tiny dither voltage D is applied to the FS to lightly change φ in step 7. The deviation values E before and after fine-tuning are calculated and used to obtain the partial derivative $(E_2 - E_1)/D$ [26, 27], which shows the relationship between $E(v_i, \Omega_i)$ and v_i , in other words, the direction of Ω_i at this moment. In step 9, we modify v_i according to the partial derivation $(E_2 - E_1)/D$, and D is subtracted so that Ω_i can return back to its original position. τ is used to tune the step size and is negative to minimize E . The four v_i ($i=1,2,3$ and 4) are adjusted one by one as described in step 10 until E is lower than the threshold E_{thr} . The four driving voltages of the FSs are kept until E exceeds E_{thr} again.

The crux of this algorithm is how to accurately calculate the feedback signal E with single photon signals. In the polarization encoding BB84 protocol, Alice randomly modulates the polarization of photons to horizontal states $|H\rangle$, vertical states $|V\rangle$, 45° states $|H+V\rangle$, and 135° states $|H-V\rangle$. The four states are combined to make two conjugate bases, which are usually named the Z basis ($|H\rangle$ and $|V\rangle$) and X basis ($|H+V\rangle$ and $|H-V\rangle$). Bob randomly selects one of the two bases to measure the photons. The tracking scheme for the two basis is identical, so that we use the Z basis to illustrate the estimation method of E . Comparing the states sent by Alice and detected by Bob, we can obtain an MM U , which can be depicted as follows:

$$U = \begin{array}{c} \text{Alice} \backslash \text{Bob} \\ \begin{array}{cc} |H\rangle & |V\rangle \\ |H\rangle & \begin{pmatrix} j_1 & j_2 \\ j_3 & j_4 \end{pmatrix} \\ |V\rangle & \end{array} \end{array} \quad (3)$$

where j_1 and j_2 (j_3 and j_4) denote the probabilities that Bob gets $|H\rangle$ and $|V\rangle$ when Alice sends $|H\rangle$ ($|V\rangle$), respectively. Normalization requires that, $j_1 + j_2 = 1$ and $j_3 + j_4 = 1$ for matrix U . Ideally, when Alice sends a $|H\rangle$ state photon, Bob will obtain a deterministic result of $|H\rangle$ when he measures the photon with the Z basis. It is similar for the other three states. Thus, a reference matrix (RM) in the ideal situation should be an identity matrix I . However, a practical QKD system will suffer from the environmental disturbance and its intrinsic noise. As a result, the measurement matrix (MM) of single photon detection results will deviate from the RM. Thus, the distance of U and I during quantum key transmission will be highly related to the rotation degree of Alice and Bob's polarization

reference frame and can be used to calculate the feedback signal E . The method we used to calculate the distance between RM and MM is described in the following equation.

$$E = \sum_i \sum_j (U_{ij} - I_{ij})^2 = 2(j_2^2 + j_3^2) \quad (4)$$

The sample size required to perform the algorithm is an important parameter, because more samples means a longer acquisition time, which will weaken the tracking capability. The final purpose of polarization-basis tracking is to minimize the QBER, which is defined as the ratio between the wrong and the total detection results when Alice and Bob select the same basis [21]. We divide the QBER into three parts as follows:

$$QBER = QBER_b + QBER_d = \frac{K_{wrong}}{K_{shift}} \quad (5)$$

where $QBER_b$ is caused by the reference frame mismatch between Alice and Bob, which we need to compensate during the QKD procedure, $QBER_d$ is caused by the intrinsic imperfections of the QKD system, such as the modulating errors and the dark counts of the single photon detectors (SPD) which is approximately 1% to 1.5% in an typical system below. K_{wrong} represents the rate of the error key after Alice and Bob compare their measurement basis, and K_{shift} is the rate of the shifted key.

We present an experiment to verify the effectiveness of our algorithm in a typical BB84 polarization encode QKD system, the system is shown schematically in Fig. 1. Alice sends Bob a sequence of photons prepared in different states, which are chosen randomly from two conjugate polarization bases, a rectilinear basis and a diagonal basis. We use a $LiNbO_3$ (lithium niobate) polarization controller to achieve the state-selection process [14, 28], with a repetition rate of 2.5 MHz. The optical component analyzer (OCA) is used to monitor the states that Alice prepares. The mean photon numbers of the laser at Alice is attenuated to 0.1 per pulse. There are two electronic polarization controllers (EPC) on Bob's side, EPC_1 and EPC_2 , for aligning the reference frame for each measuring basis separately between Alice and Bob. Each SPD in our experiment has a detection efficiency of approximately 10%.

The finite number of samples will affect the accuracy of the QBER estimation and polarization-basis tracking. A larger block size means minor deviation and a longer acquisition time. We analyzed the relationship between the sample size, the QBER, and the estimation error (discussed in detail in the supplemental materials). In our experiment, 10% of the sifted key bits (approximately 2500 bits) revealed during the post-processing [2, 3, 18] are used to estimate the polarization basis in each feedback loop, and an estimation error of less than 0.6% has been obtained when the $QBER$ is below 10%.

The Fig. 2 is the QBER of whole system during the 24 hours test time. When the polarization control is working, the QBER for the QKD system remains at a very low level in most of the test time. The average QBER is down to 2.32% and the standard derivation of QBER is 0.87%. For the real life QKD systems, in which polarization in the fiber changes slowly for most of the transit time, our strategy is effective for polarization control. Also we perform another experiment to test the feasibility of our scheme in a fast scrambling situation.

In the polarization scrambling test, we replace 50 km of telecom fiber with another EPC_3 (not show in Fig. 1). The EPC_3 is used to generate a slowly-varying polarization change by modifying the voltage applied to one of its fiber squeezers [29]. The polarization state will rotate around an axis on the *Poincaré* sphere from the state that Alice prepared to an unknown state $|\psi\rangle$ because of the scrambling of the EPC_3 . Fig. 3 shows three tests under different rotation speeds, namely 0.2° , 0.4° , 0.6° per FC (12 s in our experiment). The blue lines depict the measurements with use of the control scheme and the results without using the control scheme are depicted by red lines as comparison. Considering the periodicity of the scrambling, we erase the repeating part of the red lines and magnify parts of the blue line (200 min to 220 min) in (d), (e) and (f) for higher clarity. In three tests, when the polarization control is working, the average QBER during 10 hours are 2.65%, 2.74% and 3.29% for (a), (b) and (c). For figure (a), compared to red line, the green line maintains a very low level during the whole test time. When the scrambling angle for EPC_3 becomes bigger in (b) and (c), the QBER is steady for most of time, but there are few abrupt rises of QBER. Actually, the tracking ability of our control system is strongly limited by the long FC, when the polarization change in the fibers is abruptly-varying, our strategy might not obtain the feedback information in time. However, such events of rising rarely occur. By increasing our low system frequency (2.5 MHz), the FC can be reduced significantly and, then the tracking performance of our control scheme will be greatly enhanced [26].

In conclusion, we have proposed and experimentally demonstrated an effective single-photon level polarization tracking scheme. The feedback control parameters of the scheme are calculated using revealed and discarded sifted bits during the post-processing procedure of QKD sessions, which makes it a real-time, effective method. Although the experiment is based on the BB84 protocol, the scheme is suitable for use in various QKD systems, such as phase-encoding QKD systems and measurement-device-independent QKD systems. In our present work, the working

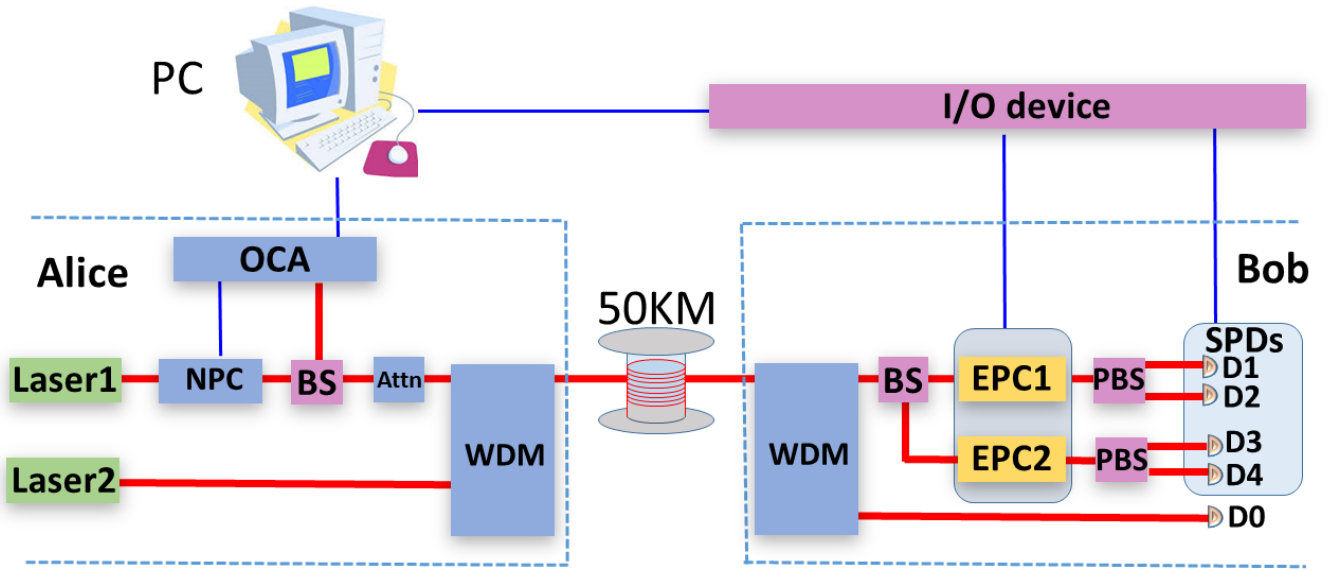


FIG. 1. (Color online) Schematic of the polarization compensation experiment set up. Thick lines (red online) represent the light path and thin lines (green online) represent electric circuits. Laser1, 1550.92 nm DFB pulse laser for quantum light; Laser2, 1549.32 nm DFB pulse laser for synchronous light; NPC, $LiNbO_3$ (lithium niobate) polarization control; BS, (50:50) beam splitter; ATTN, attenuator; EPC1, EPC2 and EPC3, electronic polarization controller; PBS, polarization beam splitter; D1, D2, D3 and D4, single photon detectors; OCA, optical component analyzer; WDM: wavelength division multiplexer; D₀, the synchronous detector; PC, personal computer.

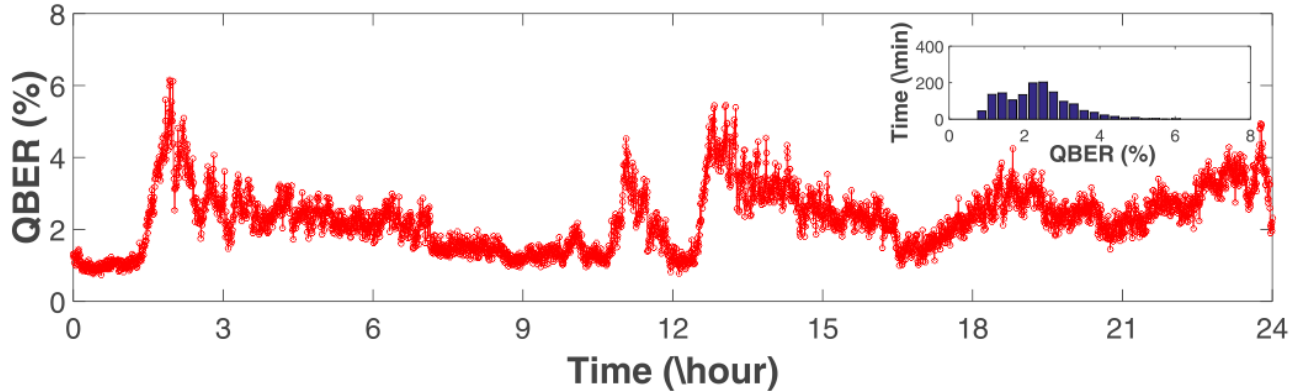


FIG. 2. (Color online) QBER of polarization-coding QKD using the polarization control strategy working during 24 hours. The inset histogram is the distribution of QBER over time.

frequency of the QKD system limits the tracking capability. Considering that the working frequency of QKD systems has previously exceeded 1GHz[30], the tracking capability of the scheme has great potential to be significantly improved[26].

This work has been supported by the National Basic Research Program of China (Grants No. 2011CBA00200 and No. 2011CB921200), the National Natural Science Foundation of China (Grant Nos. 61475148, 61575183), and the “Strategic Priority Research Program (B)” of the Chinese Academy of Sciences (Grant Nos. XDB01030100, XDB01030300).

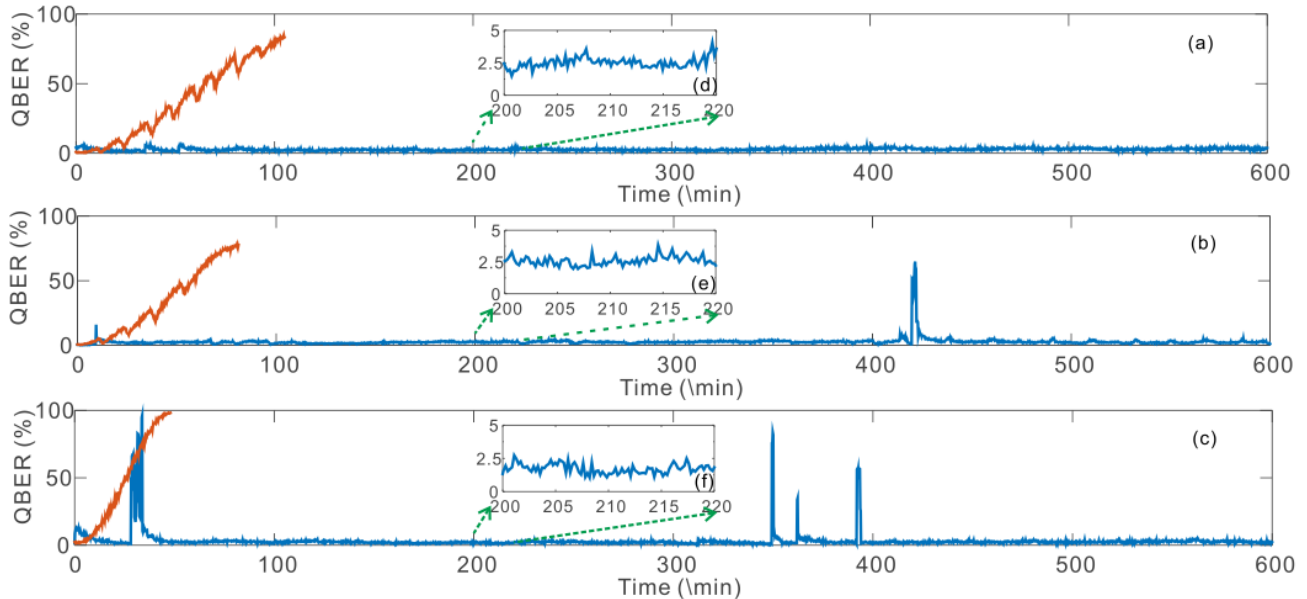


FIG. 3. (Color online) With (blue lines) and without (red lines) polarization control when dither rotation speeds are 0.2° (a), 0.4° (b), 0.6° (c) per FC. Insets (d), (e), (f) detail (200 min to 220 min) of (a), (b), (c) separately.

I. SUPPLEMENTAL MATERIAL

For our scheme, using a large enough sample size is important when tracking the polarization state, because the statistical fluctuation of the samples will weaken the reference tracking ability. Determining the required number of keys in a sample is a considerable problem. The photons, before going through the PBS with an arbitrary polarization, (we use the rectilinear base in Fig. 1 as an example), can be described by [17]

$$|\phi\rangle = \sin\theta |V\rangle + \cos\theta e^{i\phi} |H\rangle \quad (6)$$

where $|V\rangle$ and $|H\rangle$ represent the states at the exit through the vertical and horizontal ports for PBS, respectively. θ is related to the polarization projection, and ϕ is the retardation between $|H\rangle$ and $|V\rangle$. Then, we use A_1 , A_2 to represent the fraction of photons that exit through the PBS.

$$A_1 = |\langle V|\phi\rangle|^2 = 1 - \cos^2\theta \quad (7)$$

$$A_2 = |\langle H|\phi\rangle|^2 = \cos^2\theta \quad (8)$$

so the probability for detector $D1$ and $D2$ to obtain counts is [31]

$$P_1 = 1 - e^{-\eta\langle n_1\rangle} \quad (9)$$

$$P_2 = 1 - e^{-\eta\langle n_2\rangle} \quad (10)$$

where $\langle n_1\rangle = A_1\langle n\rangle$ and $\langle n_2\rangle = A_2\langle n\rangle$ are the mean number of data photons per pulse to $D1$ and $D2$ after PBS. $\langle n\rangle$ is the mean photons number per pulse for light launched by Alice. η is the overall transmission and detection efficiency between Alice and Bob

$$\eta = t_{ab}\eta_{Bob} = 10^{-\alpha l/10}\eta_{Bob} \quad (11)$$

For simplicity, we suppose the devices in our experiment are perfect, so we ignore the influence of the dark counts in the SPDs there. Where α , l and η_{Bob} are the loss coefficient in dB/Km, the length of fiber in Km and the detection efficiency of Bob's detectors, respectively. Without loss of generality, we suppose Alice only sends one polarization state $|H\rangle$. We use $QBER_t$ to represent the true error rate in the fiber. Then, we have

$$QBER_t = \langle n_1 \rangle / (\langle n_1 \rangle + \langle n_2 \rangle) = 1 - \cos^2 \theta \quad (12)$$

In our scheme, we use $QBER_e$ to estimate $QBER_t$ which is used as feedback by consuming shift keys. The sample size of consumed shift keys is B , and the counts for $D1$ and $D2$ are M and N after Alice sends B pulses to Bob. Then

$$QBER_e = M / (M + N) = M / B \quad (13)$$

M and N approach the Binomial distribution

$$P(M = m) = \binom{B}{m} P_1^m (1 - P_1)^{B-m} \quad (14)$$

$$P(N = n) = \binom{B}{n} P_2^n (1 - P_2)^{B-n} \quad (15)$$

If the sample size is infinite, we have $QBER_e = QBER_t$, but for real circumstances, there is a deviation between $QBER_e$ and $QBER_t$. According to probability theory, we know there is a 99.7% probability for $QBER_e$ to be in the section $[E(QBER_e) - 3 * \sigma_{QBER_e}, E(QBER_e) + 3 * \sigma_{QBER_e}]$, where $E(QBER_e)$ and σ_{QBER_e} are the expectation and standard deviation of $QBER_e$. Because $E(QBER_e) = QBER_t$ obviously, we use $\Delta_{QBER} = 3 * \sigma_{QBER_e}$ as the maximum offset for $QBER_e$ from $QBER_t$. According to Eq.13 and Ref.[32, 33], we have

$$\begin{aligned} \sigma_{QBER_e} &= \sqrt{Var\left(\frac{M}{B}\right)} \\ &\approx \sqrt{\frac{1}{E^2(Q')} Var(M) - 2 \frac{E(M)}{E^3(Q')} Cov(M, B) + \frac{E^2(M)}{E^4(Q')} Var(B)} \end{aligned} \quad (16)$$

where Var means variance, and Cov represent covariance. By substituting Eqs.14,15 and 16, we get

$$\Delta_{QBER} = 3 * \sigma_{QBER_e} \approx 3 * \sqrt{\frac{1}{B} * \frac{P_1 P_2 (P_1 + P_2 - 2P_1 P_2)}{(P_1 + P_2)^3}} \quad (17)$$

The maximum offset Δ_{QBER} plotted versus sample size is show in Fig. 4. Consider Eqs9, 10, 17, with $QBER = 1\%, 2\%, 3\%$ respectively and with $\eta = 10\%$, $\langle n \rangle = 0.1$ in all the case.

According the analysis above, and considering the low repetition rate of our QKD system, the sample size is chosen to be 2500 bits for one polarization base. Under these circumstances, Δ_{QBER} is under 0.6% when $QBER_t$ below 10%. If $QBER_t$ is greater than 10%, we use all the sifted keys to track the polarization reference disalignment, and it is enough for our scheme obviously. Of course, when the repetition rate rises, we can sample more bits for polarization tracking, and Δ_{QBER} will obviously be less .

-
- [1] C. H. Bennett and G. Brassard, in Proceedings of the IEEE International Conference on Computers, Systems and Signal Processing, Bangalore, India, 1984 (IEEE, New York, 1984), pp. 175-179.
 - [2] N. Gisin, G. Ribordy, W. Tittel, and H. Zbinden, Reviews of modern physics 74, 145 (2002).
 - [3] V. Scarani, H. Bechmann-Pasquinucci, N. J. Cerf, M. Duer, N. Ltkenhaus, and M. Peev, Reviews of modern physics 81, 1301 (2009).
 - [4] H.-K. Lo, M. Curty, and K. Tamaki, Nature Photonics 8, 595 (2014).
 - [5] J. Chen, G. Wu, Y. Li, E. Wu, and H. Zeng, Optics express 15, 17928 (2007).

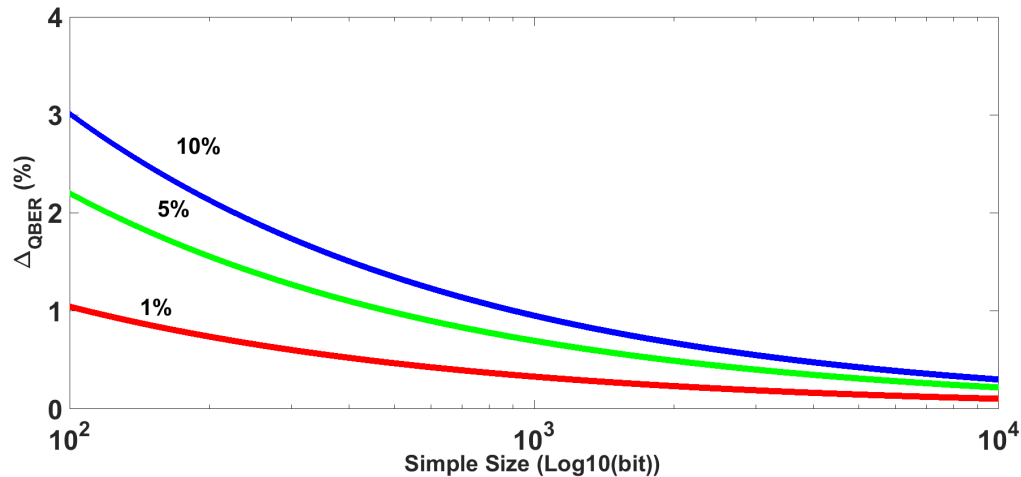


FIG. 4. (Color online) the relationship of the consumed bits used to track the SOP and the standard deviation for $QBER_e$ given different $QBER_t$.

- [6] P. A. Hiskett, D. Rosenberg, C. Peterson, R. Hughes, S. Nam, A. Lita, A. Miller, and J. Nordholt, *New Journal of Physics* 8, 193 (2006).
- [7] C. Wang, X.-T. Song, Z.-Q. Yin, S. Wang, W. Chen, C.-M. Zhang, G.-C. Guo, and Z.-F. Han, *Physical review letters* 115, 160502 (2015).
- [8] A. Muller, T. Herzog, B. Huttner, W. Tittel, H. Zbinden, and N. Gisin, 1997, *Applied Physics Letter* 70, 793795 (1997).
- [9] X.-F. Mo, B. Zhu, Z.-F. Han, Y.-Z. Gui, and G.-C. Guo, *Optics Letters*, 30, 2632-2634 (2005).
- [10] L. Ma, H. Xu, and X. Tang, Polarization recovery and autocompensation in quantum key distribution network, in *SPIE Optics+Photonics*, (International Society for Optics and Photonics, 2006), pp.630513630513.
- [11] J. Chen, G. Wu, L. Xu, X. Gu, E. Wu, and H. Zeng, *New Journal of Physics* 11, 065004 (2009).
- [12] I. Lucio-Martinez, P. Chan, X. Mo, S. Hosier, and W. Tittel, *New Journal of Physics* 11, 095001 (2009).
- [13] G. Xavier, G. V. de Faria, G. Temporo, and J. Von der Weid, *Optics express* 16, 1867 (2008).
- [14] G. Xavier, N. Walenta, G. V. De Faria, G. Temporo, N. Gisin, H. Zbinden, and J. Von der Weid, *New Journal of Physics* 11, 045015 (2009).
- [15] G. V. De Faria, J. Ferreira, G. Xavier, G. Temporo, and J. von der Weid, *Electronics Letters* 44, 1 (2008).
- [16] J. Franson and B. Jacobs, *Electronics Letters* 31, 232 (1995).
- [17] N. J. Muga, M. F. Ferreira, and A. N. Pinto *Lightwave Technology, Journal of* 29, 355 (2011).
- [18] A. Poppe, A. Fedrizzi, R. Ursin, H. Bhm, T. Lrunser, O. Maurhardt, M. Peev, M. Suda, C. Kurtsiefer, H. Weinfurter et al, *Optics Express* 12, 3865 (2004).
- [19] Z. S. Yuan, Y. A. Chen, B. Zhao, S. Chen, J. Schmiedmayer and J. W. Pan, *Nature* 454, 1098 (2008).
- [20] G. B. Xavier, F. G. Vilela, G. P. Temporo and J. P. Weid, *Optics Express* 16, 1867 (2008).
- [21] N. J. Muga, . J. Almeida, M. F. Ferreira, and A. N. Pinto, Optimization of polarization control schemes for qkd systems, in *International Conference on Applications of Optics and Photonics*, (International Society for Optics and Photonics, 2011), pp. 80013N80013N.
- [22] X. S. Yao, Fiber devices based on fiber squeezer polarization controllers,(2002). US Patent 6,493,474.
- [23] N. G. Walker and G. R. Walker, *Lightwave Technology, Journal of* 8,438 (1990).
- [24] J. B. Kuipers et al., *Quaternions and rotation sequences*, vol. 66 (Princeton university press Princeton, 1999).
- [25] M. F. Mller, *Neural networks* 6, 525 (1993).
- [26] H. Chen, M. Li, W.-Y. Liang, D. Wang, D.-Y. He, S. Wang, Z.-Q. Yin, W. Chen, G.-C. Guo, and Z.-F. Han, *Optics Communications* 358, 208 (2016).
- [27] R. Noe, H. Heidrich, and D. Hoffmann, *Lightwave Technology, Journal of* 6, 1199 (1988).
- [28] A. Hidayat, Fast endless polarization control for optical communication systems, Ph.D. thesis, Paderborn, Univ., Diss., 2008 (2008).
- [29] H. Shimizu, S. Yamazaki, T. Ono, and K. Emura, *Lightwave Technology, Journal of* 9, 1217 (1991).
- [30] Comandar, LC and Lucamarini, M and Fröhlich, B and Dynes, JF and Sharpe, AW and Tam, SW-B and Yuan, ZL and Pentyl, RV and Shields, AJ, *Nature Photonics*, Nature Publishing Group(2016).
- [31] Ma, Xiongfang and Qi, Bing and Zhao, Yi and Lo, Hoi-Kwong, *Physical Review A*, 72(1): 012326. (2005).
- [32] N. L. Johnson, *Survival models and data analysis*, vol. 74 (John Wiley , Sons, 1999).
- [33] A. Stuart, K. Ord, and S. Arnold, *Arnold: London* (1999).